

An indoor magnetic field matching positioning solution based on consumer-grade IMU for smartphone

Jian Kuang¹, Taiyu Li¹ and Xiaoji Niu^(✉)1,2

1. GNSS Research Center, Wuhan University, Wuhan, China

2. Artificial Intelligence Institute, Wuhan University, Wuhan, China

✉: corresponding author, xjniu@whu.edu.cn

Abstract: Magnetic field matching positioning (MFMP) has become one of the mainstream indoor positioning methods for mass application. However, the problem of the large workload of magnetic field mapping and the instability of the magnetometer bias remains to be solved. This paper designs an indoor MFMP scheme based on consumer-grade Inertial Measurement Units (IMUs). In the magnetic field mapping stage, the high-precision poses of the smartphone obtained by combining a foot-mounted IMU, a smartphone built-in IMU, and a few control points in the building are employed to generate a magnetic field grid map with high efficiency. In the real-time positioning stage, the relative trajectory generated by pedestrian dead reckoning (PDR) is used to improve the position discrimination of the magnetic field feature by adding spatial profile; and the differential magnetic field strength in the sensor frame (instead of in the reference frame) is used to achieve matching positioning that is immune to the magnetometer bias. The consistency of the magnetic field maps built using different smartphones show that the proposed magnetic mapping scheme achieves an average efficiency of 37 m²/min and is not affected by the mapping trajectory and walking speed. The real-time positioning results using multiple smartphones show that the proposed MFMP algorithm is barely affected by the magnetometer bias, and can achieve an average RMS value of ± 0.83 meters in a typical office scenario.

Keywords: Magnetic Matching; Pedestrian Dead Reckoning (PDR); Foot-mounted Inertial Measurement Unit (IMU); Indoor Positioning; Pedestrian Navigation

1 Introduction

The indoor geomagnetic field has the ubiquitous distortion feature due to the interference of steel materials in the building structure, which can be used for indoor positioning. Compared with the common indoor radio positioning signals (including Wi-Fi [1], Bluetooth [2], UWB [3], etc.), indoor magnetic field signals have the advantages of ubiquity, stability, and immunity from human body influence. Therefore, magnetic field matching positioning (MFMP) has become one of the mainstream indoor positioning methods for mass application [4, 5].

MFMP includes magnetic field map generation and real-time positioning parts [5, 6]. In the magnetic field map generation stage, the correlation between magnetic field features and geographic coordinates is established. Compared with the methods of point-by-point and crowdsourcing, the walking survey is the most widely used method for magnetic field map data collection by achieving a balance between accuracy and cost [6, 7]. The basic idea is the surveyors must walk along a straight line between two control points at a uniform speed, and the coordinates of the control points are determined by using professional measurement methods (e.g., total

station). However, the requirement of a straight trajectory will cause the number of control points to increase dramatically in complex indoor areas; at the same time, it is difficult for surveyors to ensure uniform straight-line walking. In general, the traditional walking survey still has the problems of heavy workload and unsure accuracy.

In the real-time positioning stage, the current position of the user is determined by calculating the similarity between the observed magnetic field feature coming from the magnetometer and the reference magnetic field feature in the magnetic field map. Dynamic time wrap (DTW) [8, 9] and particle filter (PF) [10, 11] are the two most frequently used methods in the published literature. The DTW method has the characteristics of a simple algorithm and stable positioning performance by transforming the MFMP problem into the similarity calculation of two magnetic field feature sequences. However, the real user's motion trajectories will be unpredictable in an open indoor area, then the DTW method will not work properly because there is no reference magnetic field feature sequence corresponding to the real-time user motion trajectory in the database [8]. The PF method sets a large number of particles to retain all possible positions of the user, uses the difference between the observed and the reference magnetic feature to filter out wrong particles, and obtains the current position of the user through continuous iterative calculation. The PF method has the advantages of high positioning accuracy and stable performance. However, the computational load of the PF method still needs to be further reduced for smartphones [11].

The positioning performance of the above-mentioned magnetic field matching algorithm depends on the pre-calibrated magnetometer bias. Smartphones are easily affected by nearby magnetic materials or strong currents, thereby the magnetometer bias needs to be calibrated and corrected frequently. Many researchers try to use the differential magnetic field feature in navigation coordinates (n-frame) to eliminate the effect of magnetometer bias [6, 10]. However, the assumption that the magnetometer bias is a fixed value in n-frame

does not hold in the scenario of attitude angle fluctuation. In particular, since the user often shakes when using a smartphone and the walking route is irregular, the differential magnetic field feature in n-frame cannot achieve the purpose of eliminating the magnetometer bias.

Aiming at the above-mentioned typical problems of MFMP, this paper designs an indoor MFMP solution based on consumer-grade inertial measurement units (IMUs) as follow.

- a) In the magnetic field map generation stage, a foot-mounted IMU, a handheld IMU (i.e., the smartphone built-in IMU) and combined with a few control points (e.g., as sparse as 50 meters between two adjacent control points) are used to provide the poses of the smartphone [12]. The collection of magnetic field map data can be achieved with high efficiency and sufficient precision by reducing the number of control points and releasing all user motion requirements.
- b) In the real-time positioning stage, the relative trajectory generated by pedestrian dead reckoning (PDR) is used to improve the position discrimination of the magnetic field feature, and the *differential magnetic field feature in the sensor frame* is used to achieve the magnetometer bias irrelevant matching positioning.
- c) Finally, multiple tests using various models of smartphones in real-world scenarios are conducted to verify the feasibility and localization performance of the proposed scheme.

The following content of this article is arranged as follows: Part 2 provides an overview of the proposed MFMP method, Part 3 describes the magnetic field map generation method based on the pedestrian positioning and orientation system in detail, and Part 4 describes the magnetic field matching and positioning algorithm in detail, Part 5 verifies the feasibility and effectiveness of the proposed magnetic field positioning scheme in the real environment, and Part 6 summarizes and concludes.

2 Architecture of the magnetic field positioning solution

The position error of the pure inertial navigation system (INS) based on consumer-grade IMUs will reach several meters within a few seconds, which is far from the needs of practical applications. Then, it is necessary to extract the constraint information formed by the pedestrian motion law for improving the relative positioning ability of the INS. The foot-mounted IMU utilizes the fact that the feet of pedestrians periodically contact the ground to obtain a very powerful relative positioning capability. This is the fundamental reason why the combination of foot-mounted IMU and hand-held IMU can be used to efficiently collect magnetic field vector maps [12]. At the same time, the pedestrian walking pattern is employed for controlling the velocity error of the smartphone built-in IMU-based INS, which provides reliable relative position and attitude for improving the stability and positioning accuracy of MFMP [13]. In general, the consumer-grade IMUs play an

indispensable role as the auxiliary means for the smartphone-based indoor MFMP solution.

Fig. 1 shows the flow of the MFMP scheme based on consumer-grade IMUs. The scheme can be divided into two parts:

1) Magnetic field map generation stage. A pedestrian positioning and orientation system (P-POS) composed of a foot-mounted IMU, a smartphone built-in IMU, and a few control points is used to provide high-precision pose. On this basis, a linear interpolation method is used to generate a high-precision grid map of the magnetic field vector.

2) Online positioning stage. The relative position and attitude coming from the pedestrian dead reckoning (PDR) algorithm are used for correlating the observed magnetic field strength to form a magnetic field profile [12]. Additionally, a constructed differential magnetic field profile in the sensor frame (b-frame) is used to eliminate the influence of the magnetometer bias and provide stable positioning results.

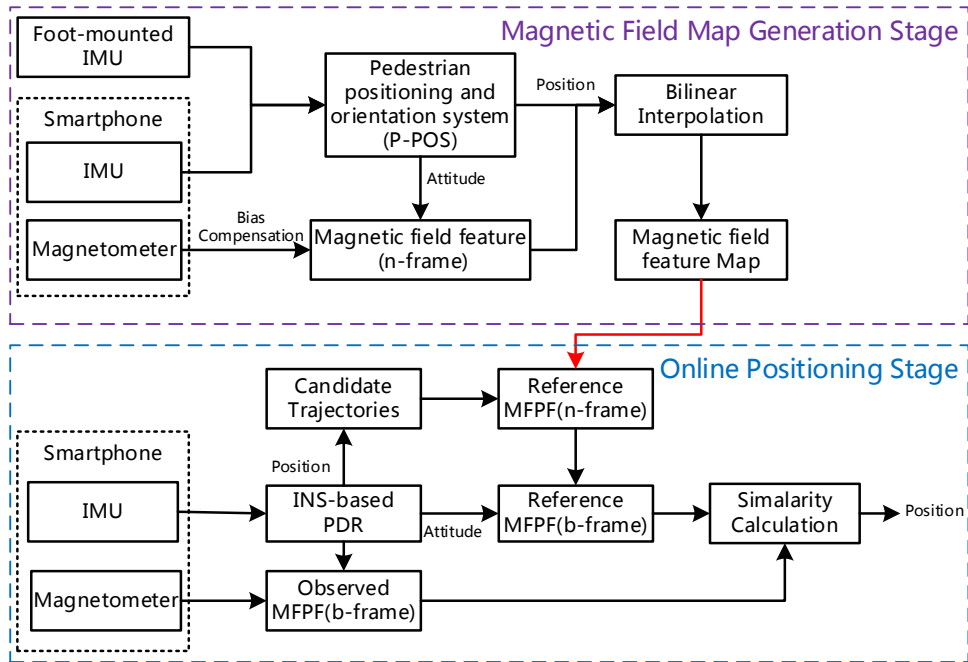


Fig. 1. The flow of the MFMP scheme based on consumer-grade IMUs.

3 Magnetic Field Map Generation Stage

The magnetic field map is the basis of the matching positioning scheme. The magnetic field map generation method is different depending on the

different application requirements, which is essentially a compromise between measurement accuracy and measurement efficiency/cost. This paper uses the P-POS-based walking survey method

to collect the magnetic field map data with high-efficiency. The proposed method reduces the number of control points and releases the movement demand of the data collectors by utilizing the superior relative positioning capability of the foot-mounted inertial navigation. After data collection, a linear interpolation method is used to generate a uniformly distributed grid map of the magnetic field vector.

Pedestrian Positioning and Orientation System (P-POS)

Fig. 2 shows the hardware setup of P-POS, including a foot-mounted IMU and a smartphone built-in IMU. P-POS can be divided into Foot-INS (Foot-mounted IMU-based Inertial Navigation System) and Foot-INS/IMU integrated. Foot-INS is a typical pedestrian dead reckoning algorithm, and the positioning error will continue to accumulate with the walking distance, the specific algorithm can be found in [14]. Foot-INS assumes that the feet of a pedestrian will periodically come into contact with the ground, that is, there is a short static state within a cycle of the footstep, as shown in Fig. 3. In the stationary state, the speed of the foot can be considered zero, which can greatly reduce the position drift error of the INS. Test results in many documents show that the positioning performance of

Foot-INS based on consumer-grade IMU fluctuates greatly, and the typical relative positioning accuracy is 0.3~3% of the total walking distance [12, 15]. To control the position drift error of Foot-INS, this scheme introduces control points (i.e., the coordinates are known) to periodically correct the position drift error of Foot-INS, and uses a reverse smoothing algorithm to further improve the positioning accuracy.

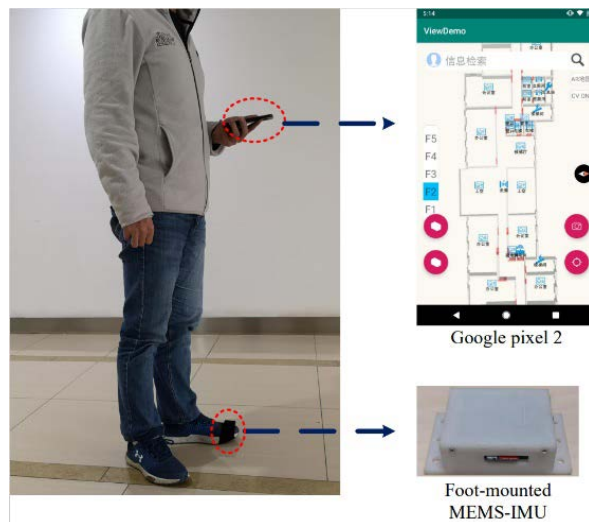


Fig. 2. The hardware setup of P-POS, including a foot-mounted IMU and a handhold smartphone built-in IMU (near the waist).

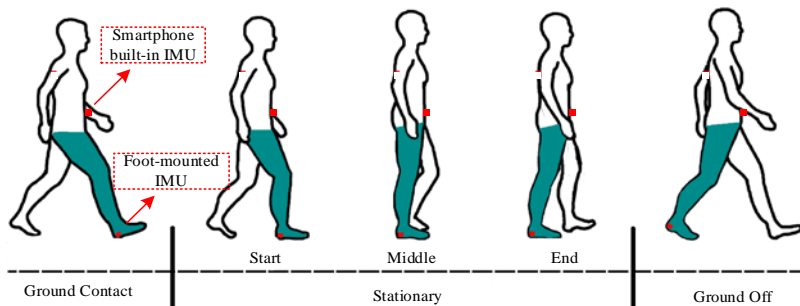


Fig. 3. Foot cycle in normal walking. The relative positional relationship between the foot and the waist in the middle of the stationary period in a step cycle that can be regarded as fixed.

Due to the large difference in magnetic field features between the foot and the waist, the trajectory coordinates generated by Foot-INS cannot be directly used to generate a magnetic field map. To obtain the precise pose of the smartphone, the position estimated by Foot-INS is used to correct the position

error of the smartphone built-in IMU. This is the core idea of the Foot-INS/IMU combination, which is similar to the GNSS/INS integrated positioning. However, the relative positional relationship between the foot and the waist is constantly changing (as shown in Fig. 3), and the position of the foot cannot

be considered equal to the position of the waist. After a thorough analysis of pedestrian walking, we found that the relative positional relationship between the foot and the waist in the middle of the stationary period in a single step cycle can be regarded as fixed. Then, the estimated position of Foot-INS can be accurately projected to the waist. [12] gives a detailed algorithm description, and its results show that the estimation accuracy of the position and attitude of the smartphone under the condition that the distance between adjacent control points is 50 meters can reach the decimeter level and the degree level, respectively.

Magnetic Field Grid Map Generation

As data collectors cannot guarantee uniform and high-density collection of magnetic field features, this paper uses the bilinear interpolation method to generate a magnetic field grid map. Many research works have shown that rigorous theoretical interpolation methods can achieve higher accuracy than bilinear interpolation[16]. However, the accuracy improvement of magnetic field maps is very limited for pedestrian localization scenarios. The magnetic field map generation includes two steps: rasterization and linear interpolation.

Rasterization: 1) Divide the test area into a uniform grid in the east-west direction and north-south direction. 2) Mark the grid where each magnetic field feature is located according to the estimated smartphone coordinates. 3) Average all the magnetic field features in a single grid.

Linear interpolation: 1) Determine the position coordinates of the grid to be interpolated (e.g., grid No. 0 in Fig. 4), and set the search radius (e.g., 1m) of the effective grid. 2) Traverse the eight directions (i.e., east, south, west, north, northwest, northeast, southeast, and southwest) of grid No. 0. The grid with a valid magnetic field feature will be marked available (e.g., the grids numbered 1~7 in Fig. 4). 3) The grid No. 3 will be eliminated based on the fact that the magnetic field features can only be interpolated; 4) The other valid grids are used for obtaining the magnetic field features of grid No. 0 by

linear interpolation. The linear interpolation formula can be expressed as

$$\mathbf{M}_0^n = \frac{\mathbf{M}_{1,5}^n + \mathbf{M}_{2,6}^n + \mathbf{M}_{4,7}^n}{3} \quad (1)$$

where

$$\mathbf{M}_{1,5}^n = \frac{d_{5-0}\mathbf{M}_1^n + d_{1-0}\mathbf{M}_5^n}{d_{1-0} + d_{5-0}}, \quad \mathbf{M}_{2,6}^n = \frac{d_{6-0}\mathbf{M}_2^n + d_{2-0}\mathbf{M}_6^n}{d_{2-0} + d_{6-0}},$$

$\mathbf{M}_{4,7}^n = \frac{d_{7-0}\mathbf{M}_4^n + d_{4-0}\mathbf{M}_7^n}{d_{4-0} + d_{7-0}}$, \mathbf{M}_i^n is the magnetic field feature in n-frame of the i-th grid,

$d_{i-0} = \sqrt{(x_i - x_0)^2 + (y_i - y_0)^2}$ is the distance between the i-th grid and the 0-th grid. In addition, the bias compensation is necessary for the observed magnetic field signal accurately reflects the real environmental magnetic field. And the simple ellipsoid fitting method is employed for calibrating the magnetometer bias [17].

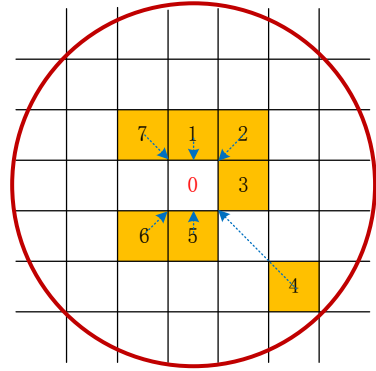


Fig. 4. Obtain a magnetic field feature by linear interpolation. The presence of two valid magnetic field features in the same direction will only be used for the interpolation method.

Compared with the traditional walking survey method, the proposed P-POS-based method has the advantages of high efficiency and high precision. This proposed solution allows the surveyor to walk on a trajectory of any shape at any walking speed, which greatly simplifies the data collection process. At the same time, the demand for the number of control points is greatly reduced, so the workload of surveyors to mark control points and the risk of incorrect control point correction are reduced. In addition, the proposed solution can provide the accurate smartphone attitude for expanding the

magnetic field map feature from 1~2 dimensions to 3 dimensions at a low cost, which supports the projection of the reference magnetic field feature from n-frame to b-frame, thus forming a matching algorithm independent of the magnetometer bias, as will mentioned in the next section.

4 Real-time Positioning Stage

The relative trajectory and attitude generated by PDR play a very important role in our MFMP algorithm. And the relative trajectory is used to correlate the magnetic field features to form a magnetic field profile, which helps to improve the position discrimination of the magnetic field features; the attitude is used to project the reference magnetic field profile from n-frame to b-frame, thereby constructing a matching algorithm independent of magnetometer bias.

Magnetic Field Profile

A magnetic field feature at a single location has low dimensionality (e.g., at most 3 dimensions) and is far from sufficient to provide accurate MFMP. Therefore, magnetic field feature time sequence (MFFTS) is widely used as an improvement scheme. As shown in Fig. 5, the user has passed through four positions A, B, C, D, etc., and combined the magnetic field features of the four points to form a magnetic field feature time sequence. However, the MFFTS still does not fully exploit the strong correlation between magnetic field features and spatial position. Therefore, this paper uses the relative trajectory generated by the PDR to correlate the MFFTS to give the relative spatial topological properties between the four positions (such as the azimuth and distance between the next point and the previous point), thereby further improving the position discrimination of the magnetic field features, called the magnetic field profile (MFP).

The INS-based PDR (INS-PDR) algorithm is used to provide the relative trajectory, which the detailed algorithm can be found in [13]. The reason to use INS-PDR is that it can achieve more robust positioning performance as the regular step-model-based PDR, while INS-PDR can also

provide 3D position, velocity, and attitude at higher frequencies (e.g., 20 Hz). Based on the relative position and attitude output by the PDR algorithm, the observed magnetic field profile can be expressed as

$$\mathbf{MFP}_{obs} = \left\{ \begin{array}{ccc} \mathbf{r}_1^n & (\mathbf{C}_b^n)_1 & \tilde{\mathbf{M}}_1^b \\ \dots & \dots & \dots \\ \mathbf{r}_k^n & (\mathbf{C}_b^n)_k & \tilde{\mathbf{M}}_k^b \end{array} \right\} \quad (2)$$

where \mathbf{r}^n is the plane position in n-frame, \mathbf{C}_b^n is the cosine matrix of the direction from b-frame to n-frame, provided by the INS-PDR algorithm, $\tilde{\mathbf{M}}^b$ is the raw observation of the magnetometer, and k is the length of a magnetic field profile. Since high sampling rate data will bring a lot of useless calculations, we use the magnetic field profile with a sampling rate of 2Hz to reduce the computational load of the matching algorithm while ensuring positioning accuracy.

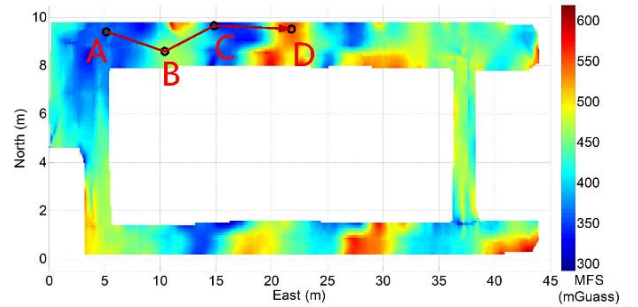


Fig. 5. Magnetic profile on magnetic field map. A magnetic field profile consists of magnetic field time series and corresponding relative trajectories.

Magnetic Field Profile Based Matching Algorithm

The basic condition for MFMP to be feasible is that the magnetic field features observed by different users on the same path are consistent. Thus, the problem of MFMP can be simplified to find the conversion relation between relative trajectory and absolute trajectory. And the conversion relationship mainly includes translation and rotation. Since the conversion relationship and absolute trajectory coordinates are parameters to be solved, they cannot be directly obtained through mathematical analysis. Therefore, we generate all possible reference

trajectories using a parametric search method and compare the similarity of the observed MFP with the reference MFP to determine the conversion relationship. Fig. 6 shows the specific process of generating candidate reference trajectory. 1) Obtain the relative trajectory S based on the relative position sequence calculated by PDR, and rotate the trajectory S around its initial point $\Delta\theta$ to obtain the trajectory S' . 2) Translate the trajectory S' in the north-south direction Δn to obtain the trajectory S'' , 3) Translate the trajectory S'' along the east-west direction translate Δe to obtain trajectory S''' .

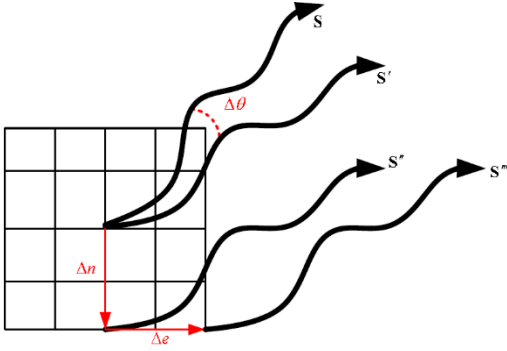


Fig. 6. The generation process of multiple candidate trajectories. All possible candidate trajectories are generated by traversing the translation parameter $(\Delta n, \Delta e)$ and rotation parameter $\Delta\theta$.

The candidate trajectory S''' can be expressed as:

$$\mathbf{r}_j^{n'} = \mathbf{C}(\Delta\theta)(\mathbf{r}_j^n - \mathbf{r}_1^n) + \mathbf{r}_1^n + \Delta\mathbf{r}^n \quad (3)$$

where $\Delta\mathbf{r}^n = [\Delta n \quad \Delta e]^T$,

$$\mathbf{C}(\Delta\theta) = \begin{bmatrix} \cos(\Delta\theta) & -\sin(\Delta\theta) \\ \sin(\Delta\theta) & \cos(\Delta\theta) \end{bmatrix},$$

$\mathbf{r}_j^{n'}$ is the coordinates of the j -th point of the candidate reference trajectory. The corresponding direction cosine matrix \mathbf{C}_b^n also needs to be adjusted accordingly

$$(\mathbf{C}_b^{n'})_j = \mathbf{C}_b^{n'}(\mathbf{C}_b^n)_j \quad (4)$$

where $(\mathbf{C}_b^{n'})_j$ is the directional cosine matrix from b-frame to n-frame corresponding to the j -th point of

the candidate reference trajectory and

$$\mathbf{C}_n^{n'} = \begin{bmatrix} \cos(\Delta\theta) & -\sin(\Delta\theta) & 0 \\ \sin(\Delta\theta) & \cos(\Delta\theta) & 0 \\ 0 & 0 & 1 \end{bmatrix}.$$

Since the magnetic field map is composed of uniformly distributed reference points, the sampling points of the candidate reference trajectory cannot be exactly coincident with the reference points. Therefore, the bilinear interpolation method is used to obtain the reference magnetic field feature with higher resolution [5], as shown in Fig. 7.

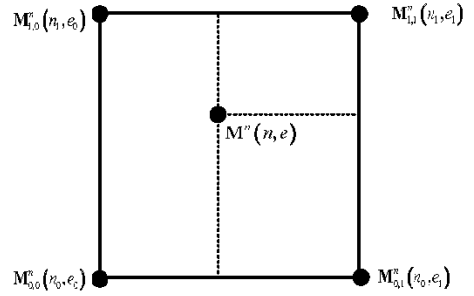


Fig. 7. Reference magnetic feature at (n, e) from the bilinear interpolation method.

A given point coordinate (n, e) , its corresponding reference magnetic field feature is

$$\mathbf{M}^n \approx \alpha_1 \mathbf{M}_{0,1}^n + \alpha_2 \mathbf{M}_{0,0}^n + \alpha_3 \mathbf{M}_{1,1}^n + \alpha_4 \mathbf{M}_{1,0}^n \quad (5)$$

where

$$\alpha_1 = \frac{(n_1 - n)(e - e_0)}{(n_1 - n_0)(e_1 - e_0)}, \alpha_2 = \frac{(n_1 - n)(e_1 - e)}{(n_1 - n_0)(e_1 - e_0)}$$

$$\alpha_3 = \frac{(n - n_0)(e - e_0)}{(n_1 - n_0)(e_1 - e_0)}, \alpha_4 = \frac{(n - n_0)(e_1 - e)}{(n_1 - n_0)(e_1 - e_0)}$$

The reference magnetic field profile can be expressed as

$$\mathbf{MFP}_{ref} = \begin{Bmatrix} \mathbf{r}_1^{n'} & (\mathbf{C}_b^{n'})_1 & \mathbf{M}_1^b \\ \dots & \dots & \dots \\ \mathbf{r}_k^{n'} & (\mathbf{C}_b^{n'})_k & \mathbf{M}_k^b \end{Bmatrix} \quad (6)$$

where $\mathbf{M}_1^b = (\mathbf{C}_b^{n'})_1^T \mathbf{M}_1^n$ is the reference magnetic field profile in b-frame.

Due to the magnetometer bias being a constant value in a short time (e.g., 15 seconds), the

Therefore, the proposed method can achieve much higher measurement efficiency than traditional methods in practical applications due to fewer control points and simpler operation procedures.

Due to the lack of a high-precision magnetic field map reference, we use the within-accuracy coincidence of the magnetic field map to evaluate the performance of the proposed method. Fig. 9 shows the magnetic field map generated using Google pixel2. The vertical axis and the horizontal axes are the north and east positions respectively, and the colors represent the values of the magnetic field feature. Subgraphs (a) ~ (c) are the north, east and down components. The magnetic field features transition smoothly with the change of the region, which is in line with the real case. Fig. 10 shows the difference between the magnetic field map using Mi-8 and Google pixel2. The differences in the magnetic field map in most areas are distributed around 0 milligauss (mGauss), indicating that the P-POS provides position and attitude with good repeatability. In addition, the difference reached about 100 mGauss in some areas. This is because the accuracy of P-POS is limited (such as decimeter level)

and there is a position projection error caused by the relative position change between the smartphone and the Foot-INS. In addition, the magnetic field feature decay with the 3rd power of the spatial distance [19], small position and attitude errors will cause obvious magnetic field feature deviation when approaching a magnetic field interference source.

To present the consistency of the magnetic maps in a quantitative way, Fig. 11 shows the cumulative density function of the difference in the magnetic field maps using two different smartphones. Table 2 shows the root mean square (RMS), 68%, and 95% of the difference in the magnetic field maps using two different smartphones. The difference in the three directions of the magnetic field maps using any two smartphones is less than 20 mGauss (RMS), and 95% of the difference is less than 40 mGauss. Compared with the noise level of magnetometers built-in most smartphones are about $\pm 10 \sim \pm 20$ mGauss, and the errors caused by P-POS and map generation algorithms are very small. Therefore, the proposed magnetic field map generation method has the characteristics of high efficiency and high precision

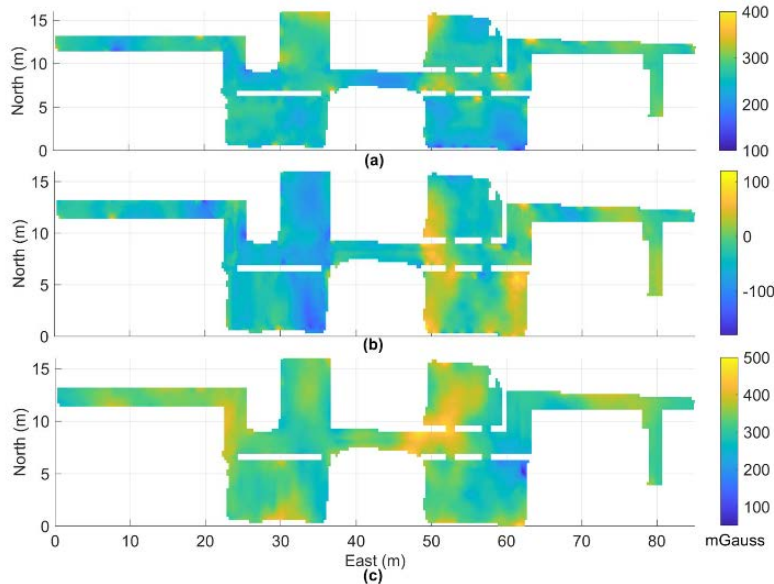


Fig. 9. Magnetic field map using Google pixel2. (a) North, (b) East, (c) Down

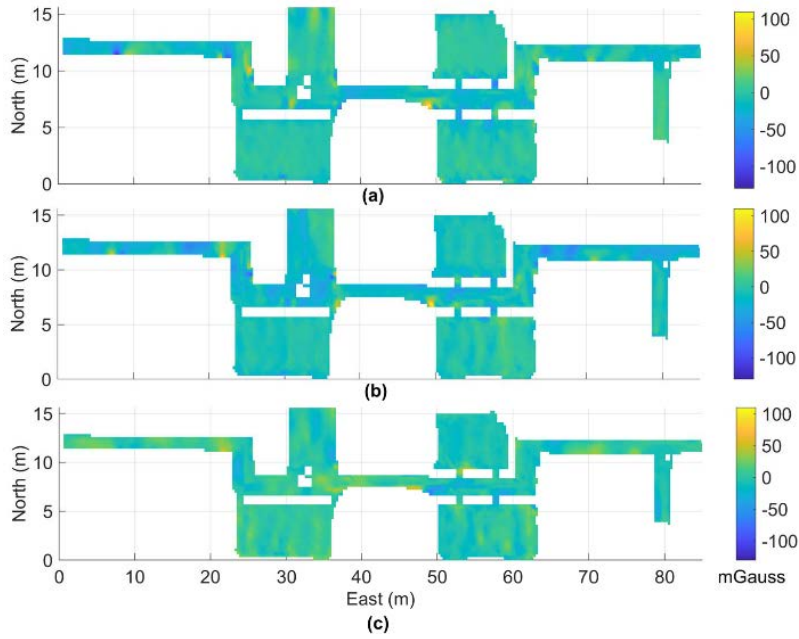


Fig. 10. The difference of two magnetic field maps using Mi 8 and Pixel 2. (a) North, (b) East, (c) Down.

Table 2. Root mean square, 68% and 95% of the difference of magnetic field maps using different smartphones (unit: mGauss)

	Mi8- Pixel3		Mi8-Pixel2		Pixel2- Pixel3	
	RMS	68%/95%	RMS	68%/95%	RMS	68%/95%
North	± 16.0	$\pm 12.1/\pm 32.3$	± 13.0	$\pm 10.1/\pm 25.2$	± 18.4	$\pm 16.2/\pm 35.6$
East	± 19.4	$\pm 16.7/\pm 39.1$	± 14.7	$\pm 13.1/\pm 28.7$	± 19.1	$\pm 18.3/\pm 36.3$
Down	± 13.6	$\pm 11.6/\pm 27.7$	± 17.0	$\pm 15.8/\pm 32.6$	± 18.4	$\pm 17.6/\pm 36.2$

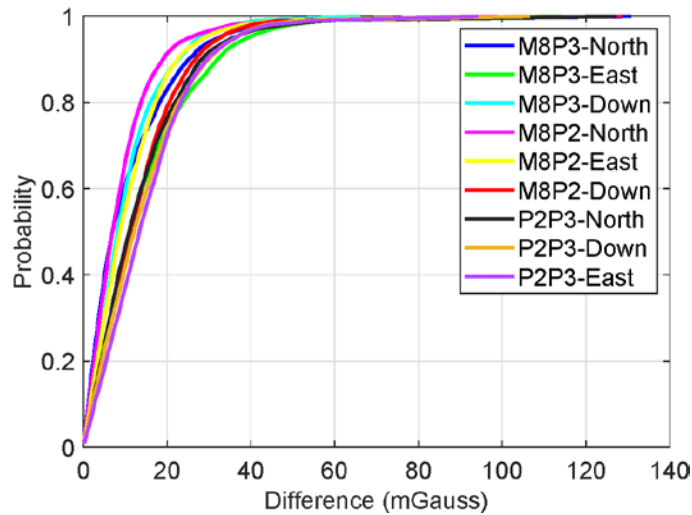


Fig. 11. The cumulative density function of the difference of three generated magnetic field maps using two different smartphones

5.3 Real-time Positioning Performance Analysis

Since the magnetic field features do not have the global positioning capability, MFMP is usually used

as an auxiliary positioning method. Here, the initial position is manually given, and WiFi/Bluetooth can be used to give a rough position (such as the position error less than 10m) for the real-time positioning

application. As the proposed algorithm is insensitive to the magnetometer bias, so the real-time positioning algorithm evaluation stage will no longer need to perform bias compensation on the magnetometer observations.

Based on the magnetic field map generated with Pixel2, we conducted 8 tests using 4 different models of smartphones (including Honor V10, Google Pixel2, Pixel3, and Mi8). To be consistent with the user movements in the real scene, the testers walked on a straight trajectory in corridor area and walk on an irregular curved trajectory in open area. Fig. 12 shows the trajectories of these 8 tests. The red line is

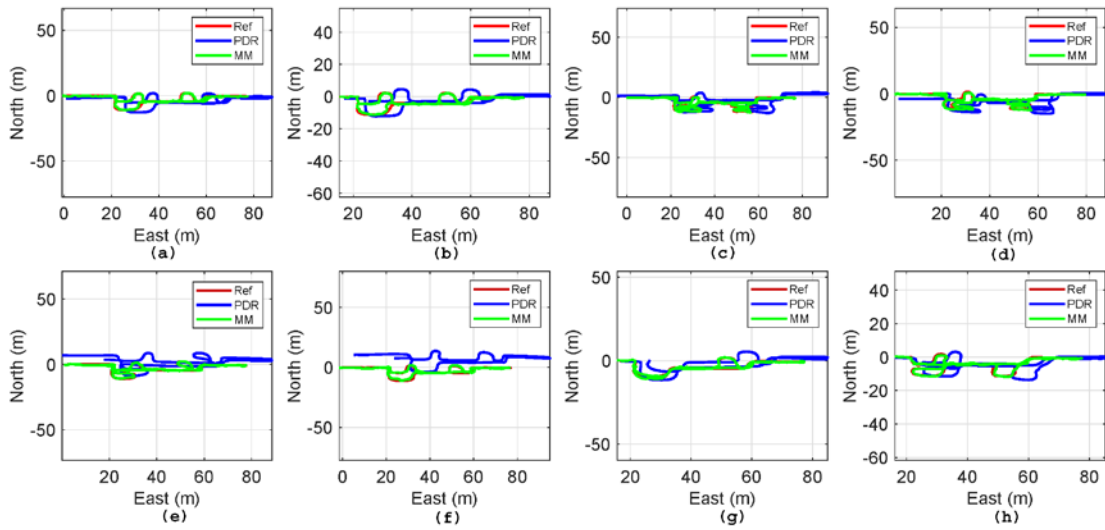


Fig. 12. The trajectories of 8 tests using 4 smartphones. (a) and (b) correspond to Honor V10, (c) and (d) correspond to Google Pixel3, (e) and (f) correspond to Mi 8, (g) and (h) correspond to Google Pixel2

Fig. 13 shows the cumulative density function of position error for 8 tests, and "V10-1" is the first test of Honor V10. The positioning errors are relatively concentrated and most of which are within 1.5 meters. Table 3 summarizes the RMS, 68% and 95% of the position error for 8 tests. The RMS of the position errors of the 8 tests distribute in $\pm 0.67 \sim \pm 1.01$ m, and the fluctuation range (i.e., 0.34m) of the positioning error is smaller than the length of a pedestrian step (about 0.6 meters). We can learn that the MFMP algorithm designed in this paper is not sensitive to the magnetometer bias, and the positioning performance difference between multiple smartphones is also small. The mean value of the RMS, 68% and 95% are ± 0.83 m, ± 0.79 m, and ± 1.60 m, respectively, which shows that the method proposed in this paper can

reach the meter-level/sub-meter-level positioning accuracy. the reference truth trajectory (given by P-POS); the blue line is the PDR trajectory, and the green line is the trajectory of MFMP. The sub-pictures (a) and (b) correspond to Honor V10, (c) and (d) correspond to Google Pixel3, (e) and (f) correspond to Mi 8, (g) and (h) correspond to Google Pixel2. The trajectories generated by the PDR in all tests have different scale and deformation error, and the trajectories of MFMP has a good degree of coincidence with the reference trajectories. We can learn that the relative trajectory and attitude with errors provided by PDR can be used to improve the performance of magnetic field matching.

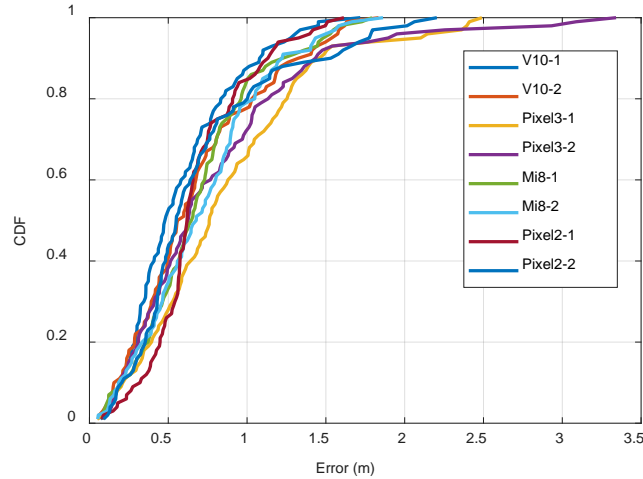
reach the meter-level/sub-meter-level positioning accuracy.

6 Conclusion and Outlook

This study proposed an indoor magnetic field matching positioning solution of smartphone based on consumer-grade IMU. The solution has greatly improved the relative positioning and attitude estimation ability of the consumer-grade IMUs by using the constraint information formed by the pedestrian movement characteristics. The magnetic field map construction efficiency and real-time positioning stability have consequently been enhanced significantly.

Table 3. RMS: 68% and 95% of positioning error of 8 tests (unit: m)

Test	V10-1	V10-2	Pix3-1	Pix3-2	Mi8-1	Mi8-2	Pix2-1	Pix2-2	Mean
RMS	± 0.67	± 0.79	± 1.01	± 0.99	± 0.78	± 0.87	± 0.74	± 0.84	± 0.83
68%	± 0.66	± 0.74	± 1.00	± 0.88	± 0.78	± 0.86	± 0.70	± 0.72	± 0.79
95%	± 1.27	± 1.53	± 2.10	± 1.89	± 1.48	± 1.43	± 1.32	± 1.77	± 1.60

**Fig. 13.** Cumulative density function of position error of 8 tests

In the magnetic field map generation stage, a P-POS is used to provide decimeter-level positioning and degree-level attitude (including roll, pitch, and heading) of the smartphone. The test results of using three smartphones to generate magnetic field maps show that the data collection efficiency of the proposed method has reached $37\text{m}^2/\text{min}$ and $55\text{m}^2/\text{min}$ maximum, and the inconsistency of the magnetic field maps using different smartphones is less than 20 mGauss (RMS).

In the real-time positioning stage, the position and attitude provided by PDR are used to improve the position discrimination of the magnetic field features and obtain the transformation relationship from the navigation frame to the sensor frame, so that the differential MFP in b-frame can be used for eliminating the impact of the magnetometer bias. The results from 8 field tests using 4 models of smartphones showed the positioning errors between ± 0.67 and ± 1.01 meters, reaching an average RMS value of ± 0.83 meters. The experimental results have completely verified that the MFMP method proposed in this study is immune to the magnetometer bias,

and there is no significant difference in positioning performance between different models of smartphones.

Because the smartphone-based indoor MFMP scheme proposed in this study is highly dependent on the stability of the PDR, we will focus on automatically monitoring the integrity of the PDR and adapting it to a variety of typical smartphone usage modes in the future, such as texting, calling, and swinging. More importantly, we will explore the method of generating magnetic field maps based on crowdsourced data to further reduce the cost of the whole solution.

Remark: This paper has been originally published in the proceeding of China Satellite Navigation Conference (CSNC 2021).

References:

- [1]. Zhuang, Y. and N. El-Sheimy, Tightly-Coupled Integration of WiFi and MEMS Sensors on Handheld Devices for Indoor Pedestrian Navigation. *IEEE Sensors Journal*, 2015. 16(1): p. 224-234.
- [2]. Zhuang, Y., et al., Smartphone-based indoor

localization with bluetooth low energy beacons. *Sensors*, 2016. 16(5): p. 596.

[3]. Van Herbruggen, B., et al., Wi-PoS: A Low-Cost, Open Source Ultra-Wideband (UWB) Hardware Platform with Long Range Sub-GHz Backbone. *Sensors*, 2019. 19(7): p. 1548.

[4]. Lin, Y., et al., Autonomous aerial navigation using monocular visual-inertial fusion. *Journal of Field Robotics*, 2018. 35(1): p. 23-51.

[5]. Kuang, J., et al., Indoor Positioning Based on Pedestrian Dead Reckoning and Magnetic Field Matching for Smartphones. *Sensors*, 2018. 18(12): p. 4142.

[6]. Li, Y., Integration of MEMS Sensors, WiFi, and Magnetic Features for Indoor Pedestrian Navigation with Consumer Portable Devices. 2016, University of Calgary.

[7]. Jung, S.H., B.C. Moon and D. Han, Performance Evaluation of Radio Map Construction Methods for Wi-Fi Positioning Systems. *IEEE Transactions on Intelligent Transportation Systems*, 2017. PP(99): p. 1-10.

[8]. Shu, Y., et al. Last-Mile Navigation Using Smartphones. in *International Conference on Mobile Computing and NETWORKING*. 2015.

[9]. Subbu, K.P., B. Gozick and R. Dantu, LocateMe- Magnetic Fields Based Indoor Localization Using Smartphones. *ACM Transactions on Intelligent Systems and Technology*, 2013. 4(4): p. 1-27.

[10]. Kim, B. and S. Kong, Indoor Positioning based on Bayesian Filter using Magnetometer Measurement Difference, in *IEEE Vehicular Technology Conference Proceedings*. 2015.

[11]. Shi, L., M. Yu and W. Yin, PDR/Geomagnetic Fusion Localization Method Based on AOFA Improved Particle Filter. *IEEE Transactions on Instrumentation and Measurement*, 2021.

[12]. Niu, X., et al., A Novel Position and Orientation System for Pedestrian Indoor Mobile Mapping System. *IEEE Sensors Journal*, 2021. 21(2): p. 2104-2114.

[13]. Kuang, J., X. Niu and X. Chen, Robust Pedestrian Dead Reckoning Based on MEMS-IMU for Smartphones. *Sensors*, 2018. 18(5): p. 1391.

[14]. Foxlin, E., Pedestrian tracking with shoe-mounted inertial sensors. *IEEE COMPUTER GRAPHICS AND APPLICATIONS*, 2005. 25(6): p. 38-46.

[15]. Liu, T., et al., A Simple Positioning System for Large-Scale Indoor Patrol Inspection Using Foot-Mounted INS, QR Code Control Points, and Smartphone. *IEEE Sensors Journal*, 2021. 21(4): p. 4938-4948.

[16]. Hensel, S., et al., Application of Gaussian Process Estimation for Magnetic Field Mapping. 2021, Springer International Publishing: Cham. p. 284-298.

[17]. Tabatabaei, S., A. Gluhak and R. Tafazolli, A Fast Calibration Method for Triaxial Magnetometers. *IEEE Transactions on Instrumentation & Measure...*, 2013.

[18]. Liu, G., et al., Human-interactive Mapping Method for Indoor Magnetic Based on Low-cost MARG Sensors. *IEEE Transactions on Instrumentation and Measurement*, 2021: p. 1-1.

Authors



Jian Kuang is an Associate Researcher Fellow of GNSS Research Center at Wuhan University in China. He got his Ph.D. and bachelor degrees from Wuhan University in 2019 and 2013 respectively. Her research interest includes pedestrian navigation, vehicle positioning, magnetic field matching, and multi-system fusion positioning.



Taiyu Li received the B.Eng. degree in Geodesy and Survey Engineering from China University of Mining and Technology, Xuzhou, China, in 2019. He is currently a Master student in the GNSS Research Center, Wuhan University, Wuhan, China. His research interests focus on pedestrian navigation and indoor positioning.



Dr. Xiaoji Niu is a Professor of GNSS Research Center at Wuhan University in China. He got his Ph.D. and bachelor degrees from Tsinghua University in 2002 and 1997 respectively. He did

post-doctoral research at the University of Calgary and worked as a senior scientist in SiRF Technology Inc. Dr. Niu leads a multi-sensor navigation group focuses on GNSS/INS integrations, low-cost navigation sensor fusion, and the relevant new applications. Dr. Niu has published 100+ academic papers and own 30+ patents.